

# Research on the Spatial Coherent Characteristics of High Power VCSEL

Jia Peng<sup>1,2</sup> Qin Li<sup>1</sup> Cui Jinjiang<sup>3</sup> Li Xiushan<sup>1,2</sup> Chen Yongyi<sup>1</sup> Zhang Jianwei<sup>1</sup>  
Zhang Jian<sup>1</sup> Zhang Xing<sup>1</sup> Ning Yongqiang<sup>1</sup>

<sup>1</sup> State Key Laboratory of Luminescence and Application, Changchun Institute of Optics,  
Fine Mechanics and Physics, Chinese Academy of Sciences, Changchun, Jiling 130033, China

<sup>2</sup> University of Chinese Academy of Sciences, Beijing 100049, China

<sup>3</sup> Suzhou Institute of Biomedical Engineering and Technology, Chinese Academy of Sciences,  
Suzhou, Jiangsu 215163, China

**Abstract** The spatial coherence properties of high power vertical cavity surface emitting lasers (VCSELs) are studied based on the theorem of partially coherent light proposed by Van Cittert-Zernike. The interference stripe patterns are gauged using the Young's double-slit experiment for the devices of 980 nm wavelength VCSEL single emitters. Then interference patterns are switched to grayscale by intensity distribution patterns for data collection. In this paper, the integral average value method is proposed to calculate the degree of spatial coherence. The proposed integral average value method and traditional average method are used respectively to calculate the light intensity of the pattern. The results are compared with those calculated by the theoretical value of Van Cittert-Zernike theorem. The VCSEL optical apertures' influence on coherent characteristics are also discussed. The experimental results show that, a relative error within 2.5% ~ 9.4% is reached by our integral average value method. On the contrary, a relative error of 7.5% ~ 67.4% are got from the traditional average method. Apparently, traditional average value method causes the error generally 1.5 ~ 27 times worse than our integral average value method. Moreover, for single emitter VCSELs with optical aperture from 200  $\mu\text{m}$  to 500  $\mu\text{m}$ , the smaller the optical aperture are, the larger the coherent degrees (between 0.731 ~ 0.426) are. The conclusion can be widely used on theoretical and experimental design for VCSEL coherent arrays.

**Key words** coherence optics; coherent characteristics; double-slit; vertical cavity surface emitting laser; degree of spatial coherence(DSC)

**OCIS codes** 140.5960; 140.7260

## 大功率 VCSEL 器件的空间相干性的研究

贾 鹏<sup>1,2</sup> 秦 莉<sup>1</sup> 崔锦江<sup>3</sup> 李秀山<sup>1,2</sup> 陈泳屹<sup>1</sup> 张建伟<sup>1</sup> 张 建<sup>1</sup> 张 星<sup>1</sup> 宁永强<sup>1</sup>

(<sup>1</sup>中国科学院长春光学精密机械与物理研究所发光学及应用国家重点实验室, 吉林 长春 130033)  
(<sup>2</sup>中国科学院大学, 北京 100049; <sup>3</sup>中国科学院苏州生物医学工程技术研究所, 江苏 苏州 215163)

**摘要** 由 Van Cittert-Zernike 提出的部分相干光定理出发,研究了大功率垂直腔面发射激光器(VCSEL)及其列阵器件的空间相干特性。采用杨氏双缝干涉实验装置得到 980 nm 波段 VCSEL 单管器件的干涉条纹图样,再将干涉图样转换进行灰度读取处理得到光强分布图样,最后分别采用积分法和平均值法对光强图样进行计算,所得结果与由 Van Cittert-Zernike 定理所得的空间相干度理论值进行对比,并讨论了 VCSEL 器件发光孔径对其空间相干度的影响。实验结果表明提出的积分法计算出的空间相干度与理论值的误差在 2.5% ~ 37.4%。而常用的平均值法所得结果与理论值的误差为 7.5% ~ 120.5%。可见,传统算法误差普遍大于积分算法 1.5 ~ 27 倍。出光孔径在 200 ~ 500  $\mu\text{m}$  的单管 VCSEL 器件相干度在 0.731 ~ 0.426 之间,且发光孔径越小,其相干度越大。分析了积分平

收稿日期: 2014-06-09; 收到修改稿日期: 2014-07-17

基金项目: 国家自然科学基金(61234004, 61106068, 61176045, 61306086, 61306070)、吉林省科技厅项目(20140101172JC, 20130206006GX)、江苏省自然科学基金(BK2012188)

作者简介: 贾 鹏(1986-),男,博士研究生,主要从事高功率 DFB 激光器及其相干列阵等方面的研究。

E-mail: modou1986@163.com

导师简介: 秦 莉(1969-),女,研究员,博士生导师,主要从事半导体激光技术及应用等方面的研究。

E-mail: qinl@ciomp.ac.cn(通信联系人)

均值法和传统平均值法的优劣及 VCSEL 器件出光孔径对相干特性的影响,为 VCSEL 相干阵列的设计提供了必要的理论和实验依据。

**关键词** 相干光学;相干特性;双缝干涉;垂直腔面发射半导体激光器;空间相干度

**中图分类号** TN248.4 **文献标识码** A **doi**: 10.3788/CJL201441.1202007

## 1 Introduction

Vertical cavity surface emitting laser (VCSEL) [1-4] is a kind of semiconductor laser which has a low threshold current and circular symmetric output light spot owing to microcavity effect [5]. Its coherent characteristics are of great importance in many application fields such as communication, medical care, aerospace and so on [6-7]. On one hand, it is widely accepted that, VCSELs with milliwatt-output corresponding to a few-micron optical aperture have a high degree of coherence, since the cavity only supports base transverse mode [8-9]. On the other hand, for a watt-output high power VCSEL corresponding to an optical aperture about a few hundred microns, the degree of coherence is heavily reduced as a result of the coexistence of multiple transverse modes in the cavity [8].

The past work on the coherent characteristics of VCSEL [10-12] was basically qualitatively illustrated by far

field distribution and the spectral characteristics. However, these parameters are apparently inadequate for a quantitative illustration on the degree of coherence. In this paper, we firstly proposed an integral average value method (IAVM) based on the Young's interference experiment and spatial coherence theory [13], which should be suitable for analyzing the degree of spatial coherence (DSC) for high power VCSELs. Comparing with our IAVM, the traditional analysis method [traditional average value method (TAVM)] showed a relatively 1.5~27 times larger error.

## 2 Theorem of coherence

This article mainly discussed the DSC of high power VCSEL devices. Spatial coherence is defined with the light wave superposition effect, which is shown in Fig. 1 [13].

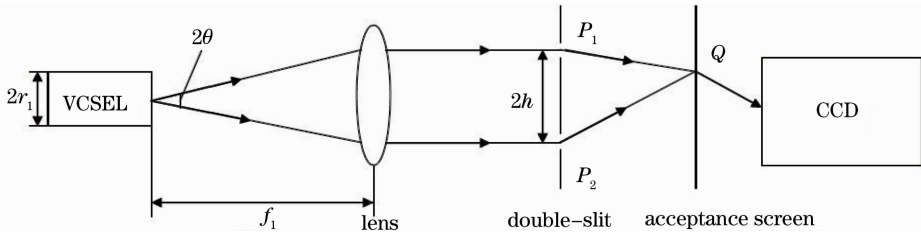


Fig.1 Experimental test equipment

The circular optical aperture of VCSEL device can be regarded as a stationary optical source. According to the Van Cittert-Zernike theorem and Wolf theorem [13-15], considering two-beam interference with partially coherent light at point Q in a stationary optical field, the interference intensity at Q is given by

$$I(\phi, r_1) = 2 \left[ \frac{2J_1(\nu)}{\nu} \right]^2 \left\{ 1 + \left| \frac{2J_1(\mu)}{\mu} \right| \cos[\beta_{12}(\mu) - \delta] \right\}, \quad (1)$$

$$\mu = \frac{2\pi}{\lambda} r_1 \sin(2\theta) = \frac{2\pi}{\lambda} r_1 \frac{2h}{f_1}, \quad \nu = \frac{2\pi}{\lambda} \alpha \sin \phi, \quad (2)$$

$\beta_{12}$  is the initial mean phase and  $\delta$  is the effective phase difference between the two beams.  $2\theta$  is the full divergence angle of VCSEL,  $2h$  is the separation between two slits,  $r_1$  is the optical aperture of VCSEL,  $f_1$  is the focal length of the optical lens,  $\lambda$  is the mean wavelength,  $\alpha$  is half width of one slit,  $\phi$  is the azimuth angle of point Q in the focal plane.

For a fixed  $r_1$ ,  $I(\phi, r_1)$  represents a curve with a series of maxima and minima situated between the two envelopes:

$$I_{\max}(\phi, r_1) = 2 \left[ \frac{2J_1(\nu)}{\nu} \right]^2 \left[ 1 + \left| \frac{2J_1(\mu)}{\mu} \right| \right], \quad I_{\min}(\phi, r_1) = 2 \left[ \frac{2J_1(\nu)}{\nu} \right]^2 \left[ 1 - \left| \frac{2J_1(\mu)}{\mu} \right| \right]. \quad (3)$$

In the high power VCSELs, the intensities of the two beams should be equal, so that the visibility  $\nu$  of the stripes is

$$\nu = \frac{I_{\max} - I_{\min}}{I_{\max} + I_{\min}} = |\gamma_{12}(0)| = \left| \frac{2J_1(\mu)}{\mu} \right| = \left| \frac{2 \sum_{m=0}^{\infty} \frac{(-1)^m (\mu)^{2m+1}}{2^{2m+1} m! (m+1)!}}{\mu} \right|. \quad (4)$$

The traditional coherence degree measurement method is called the traditional average value method [TAVM] [16] [Fig. 2 (a)]. This method need to measure each  $I_{\max}$  and  $I_{\min}$  of interference stripes. From formula (4), we can get each visibility of interference stripes. An average visibility can be achieved using all these visibilities. Yet the results are often larger than the theoretical value [16].

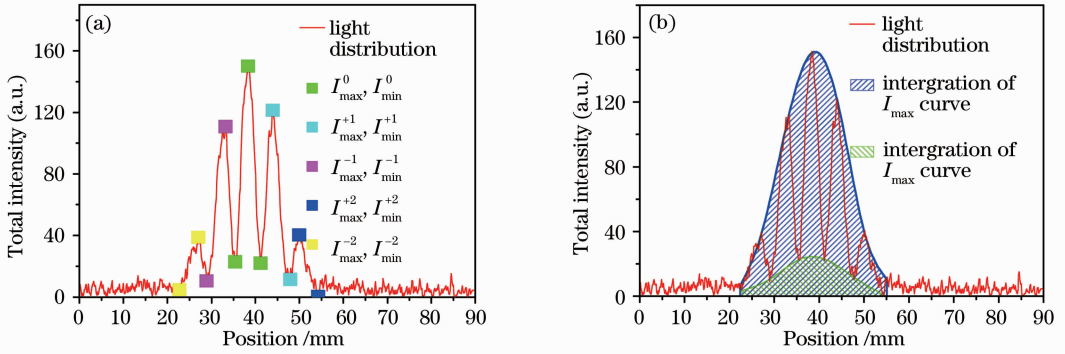


Fig. 2 Schematic diagram of TAVM(a) and IAVM(b)

In this paper, we propose the IAVM, to calculate the measured value of the DSC [Fig. 2 (b)]. The IAVM is, we first fit out the  $I_{\max}$  and  $I_{\min}$  envelope curves using a set of  $I_{\max}$  and  $I_{\min}$  experimental values. According to the formula (3), the curves of  $I_{\max}$  and  $I_{\min}$  are the maximum and minimum envelope curve of the distribution curve of  $I_Q$ . An average could be achieved by a great amount of calculations using values on the fitting curves. So we simplified this step by the integration of all the points on the curves of  $I_{\max}$  and  $I_{\min}$  as  $S_{\max}$  and  $S_{\min}$ . Then  $S_{\max}$  and  $S_{\min}$  are taken into formula (4) to calculate visibility. We get

$$\nu = \frac{S_{\max} - S_{\min}}{S_{\max} + S_{\min}} = \frac{\int I_{\max} - \int I_{\min}}{\int I_{\max} + \int I_{\min}}. \quad (5)$$

### 3 Experimental measurement and data analysis

Our experiment is set up as Fig. 1. VCSELs are collimated by an optical lens, followed by the adjustable double slits. A same constant current electrical source is applied and optical power is measured. The position of the receiving screen is adjusted until interference stripes are clear and stable on the translucent receiving screen. A

Table 1 Theoretical values and experimental values of DSC of (a)~(e) groups VCSEL devices by IAVM and traditional average value method

Number	Theoretical value of DSC	Experimental value of DSC			
		IAVM		TAVM	
		DSC of IAVM	Relative error	DSC of TAVM	Relative error
a	0.756	0.72	4.8%	0.813	7.5%
b	0.699	0.731	4.6%	0.783	12.1%
c	0.534	0.513	3.9%	0.78	46.3%
d	0.466	0.426	9.4%	0.666	42.3%
e	0.443	0.432	2.5%	0.724	67.4%

Table 2 Theoretical calculation parameters of (a)~(e) groups 980 nm VCSELs

Number	Optical aperture / $\mu\text{m}$	$r_1$ / $\mu\text{m}$	$f_1$ /cm	$2h$ /nm	$\mu$ (a. u.)
a	200	100	7.6	120	1.46
b	300	150	7	120	1.65
c	400	200	7.3	120	2.12
d	400	200	6.7	120	2.31
e	500	250	8.1	120	2.37

CCD camera is utilized to collect the intensity distribution of the stripes, for further calculation and analysis.

Five high-power 980nm VCSEL devices made in our laboratory are selected. The device parameters are shown in Table 1. The five devices (a)~(e) are tested under a current injection 1.5 times of threshold.

In Fig. 3, (a1)~(e1) show the interference stripes and (a2)~(e2) give the corresponding intensity distributions of the five VCSELs respectively. Both two beam interference and slit diffraction exist, as shown in (a1)~(e1). The level 0 light intensity is the strongest stripe at the center. Level  $\pm 1$ ,  $\pm 2$  stripes distribute at two sides and darken gradually [17].

Figure 3 (a2)~(e2) are the corresponding results transferred from the stripes' intensities from Fig. 3 (a1)~(e1) via Matlab respectively. The envelope curve fittings are carried out from  $I_{\max}$  and  $I_{\min}$ , shown in Fig. 3 (a2)~(e2). The visibilities are calculated using the formula (5), and the DSCs are obtained. The results are shown in Table 1 and Fig. 4.

In order to verify the validity of our IAVM, theoretical analysis according to formulas (2) and (3) are done according to our experimental results. The  $2h$ ,  $f_1$  and  $r_1$ , the corresponding  $\mu$  and optical apertures are given in Table 2.

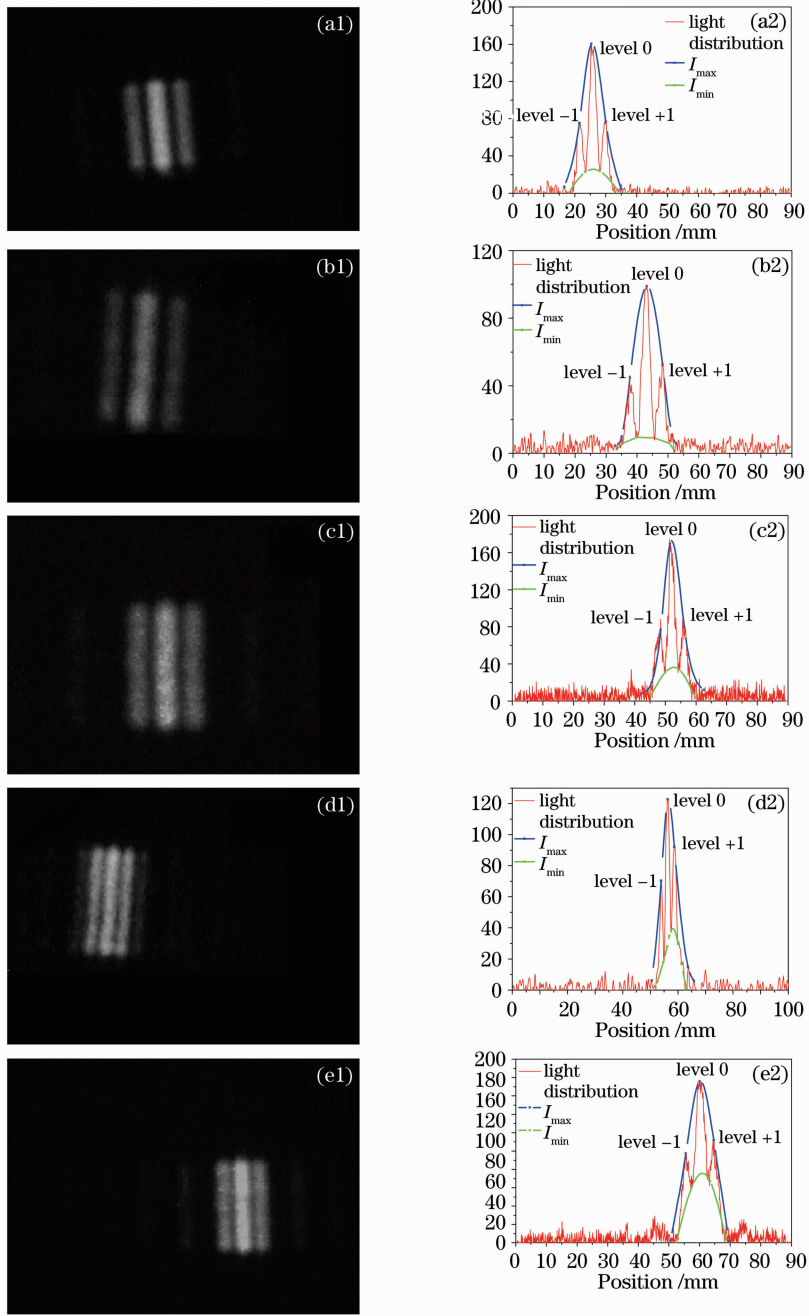


Fig.3 Interference stripes (a1)~(e1) and intensity distributions of interference stripes (a2)~(e2) for the five 980 nm VCSELs

In Table 1, the results of five sets of data using the two methods are compared with theoretical calculation results. We found that when optical aperture increases, the DSC of VCSELs became smaller. This is because when the optical aperture of VCSELs become larger, the limitation for transverse mode become worse. When the number of transverse mode of VCSELs increases, the DSC of VCSELs would become smaller. In data set (a), the relative error of traditional method is 7.5%, comparing with an error of 4.8% using the IAVM which is 1.5 times smaller. However in data set (b), it is 12.1% for TAVM comparing with 4.6% for IAVM, 2.6 times smaller. This unusual result is brought by  $f_1$  of

(b) set with a measurement error in the experiment. The  $f_1$  is measured each time when the sharpness of interference fringes are stable and clear on the computer screen transferred from the CCD camera. Certain measurement errors are inevitable when judging the sharpness. A considerable measurement error  $f_1$  of (b) would cause a decreased value of  $I_{\min}/I_{\max}$  of level 0,  $\pm 1$ ,  $\pm 2$  stripes. According to the formula (4), the measurement DSC of (b) would increase when the value of  $f_1$  slants big.

In data set (c), a relative error of TAVM is 46.3%, comparing with 3.9% for IAVM, which is 11.8 times smaller. In data set (d), the relative error of TAVM is

42.3%, comparing with 9.4% for IAVM, which is 4.5 times smaller. In data set (e), the relative error of TAVM is 67.4%, comparing with 2.5% for IAVM, which is 27 times smaller. We found that the Integration average value of DSC of (c) is greater than the value of (e), but the integration average value of DSC of (d) is smaller than the value of (e). This is because, a certain etching process error occurs: optical apertures of (d) deviate more from 400  $\mu\text{m}$ , it would lead to a measurement error.

Apparently, errors of TAVM are generally 1.5 ~ 27 times larger than our IVAM. These differences are because, in TAVM, only a few  $I_{\text{max}}$  and  $I_{\text{min}}$  are taken into account to calculate visibility of interference stripes [Fig. 2 (a)]. The system error and experimental noise which would lead to the worse results and larger error, tend to affect much more apparently than our IVAM. IVAM uses fitting curves of  $I_{\text{max}}$  and  $I_{\text{min}}$  to determine the  $I_{\text{max}}$  value ( $S_{\text{max}} = \int I_{\text{max}}$ ) and  $I_{\text{min}}$  value ( $S_{\text{min}} = \int I_{\text{min}}$ ), which would be a more reasonable model to calculate average value [Fig. 2 (b)]. The individual value difference appeared in the process would affect little on the final results. From the analysis above, the IVAM would be more reasonable in calculating the spatial coherence degree for VCSEL devices rather than the TAVM obviously.

In Fig. 4, we find that the relative error of IAVM decrease from 4.8% to 2.5%, but the relative error of TAVM increase from 7.5% to 67.5%. It is because that the five VCSEL devices are made by the wet etching technology, it would lead to an error value  $2\Delta r$  between the real value of optical aperture and the designed value of optical aperture. Under the same process condition, the  $2\Delta r$  values were more or less the same, about 10  $\mu\text{m}$ . We find that as optical aperture value  $2r_1$  of (a) ~ (e) devices increases from 200  $\mu\text{m}$  to 500  $\mu\text{m}$ , the relative error value  $2\Delta r/(2r_1)$  fell from 5% to 2%. According to the formulas (2) and (4), the error of  $\mu$  value correspondingly decreased. The error

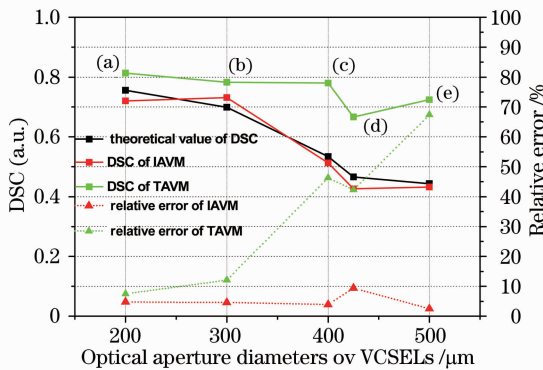


Fig. 4 Comparison diagram of experimental values of IAVM and TAVM and theoretical values and relative error of IAVM and TAVM of (a) ~ (e) groups VCSEL devices

value between DSC of IVAM and theoretical value of DSC will be smaller and smaller.

In the calculation process of TAVM, we find that: if only the level 0 interference stripe is taken into account, the DSC is not too much larger than the theoretical value of DSC. But if all interference stripes are taken into account to measure the average visibility, the relative error of TAVM will become larger, and it will grows larger and larger as optical aperture value of (a) ~ (e) devices increases from 200  $\mu\text{m}$  to 500  $\mu\text{m}$ . Higher-level interference stripes tend to bring more error for the value of DCS.

## 4 Conclusion

Theoretical analysis and experimental measurements were carried out to describe the DSC for partially coherence light in high-power VCSEL single emitters. We proposes IAVM based on Young's double-slit experiment for quantitative description. Compared with our IAVM, the TAVM shows a relatively larger error; for more than 1.5 ~ 27 times. From the analysis above, it will be reasonable to use our IAMV to get a more accurate description of DSC.

## References

- Ning Yongqiang, Zhang Xing, Qin Li, *et al.*. High-power high beam quality vertical-cavity surface-emitting lasers[J]. Infrared and Laser Engineering, 2012, 41(12): 3219 - 3225.  
宁永强, 张星, 秦莉, 等. 高光束质量大功率垂直腔面发射激光[J]. 红外与激光工程, 2012, 41(12): 3219 - 3225.
- Liu Di, Ning Yongqiang, Zhang Jinlong, *et al.*. High-power InGaAs/GaAsP strained quantum well vertical-cavity surface-emitting laser array[J]. Optics and Precision Engineering, 2012, 20(10): 829 - 834.  
刘迪, 宁永强, 张金龙, 等. 高功率 InGaAs/GaAsP 应变量子阱垂直腔面发射激光器阵列[J]. 光学精密工程, 2012, 20(10): 829 - 834.
- Shi Jingjing, Qin Li, Ning Yongqiang, *et al.*. 850 nm vertical cavity surface-emitting laser arrays [J]. Optics and Precision Engineering, 2012, 20(1): 17 - 23.  
史晶晶, 秦莉, 宁永强, 等. 850 nm 垂直腔面发射激光器阵列[J]. 光学精密工程, 2012, 20(1): 17 - 23.
- Zhang Jianwei, Ning Yongqiang, Zhang Xing, *et al.*. Gain-cavity mode detuning vertical cavity surface emitting laser operating at the high temperature [J]. Chinese J Lasers, 2013, 40(5): 0502001.  
张建伟, 宁永强, 张星, 等. 增益-腔模失配型高温工作垂直腔面发射半导体激光器[J]. 中国激光, 2013, 40(5): 0502001.
- Zhang Xing, Ning Yongqiang, Zeng Yugang, *et al.*. Optimization of element structure in 980 nm high-power vertical-cavity surface-emitting laser array[J]. Optics and Precision Engineering, 2011, 19(9): 2014 - 2022.  
张星, 宁永强, 曾玉刚, 等. 980 nm 高功率垂直腔面发射激光阵列的单元结构优化[J]. 光学精密工程, 2011, 19(9): 2014 - 2022.
- Mao M, Xu C, Kan Q, *et al.*. High beam quality of in-phase coherent coupling 2-D VCSEL arrays based on proton - implantation[J]. Photon Technol Lett, 2014, 26(4): 395 - 397.
- Zhang Jinsheng, Ning Yongqiang, Zhang Jinlong, *et al.*. Optimization of electric field intensity distribution on high power semiconductor laser facet film [J]. Chinese J Lasers, 2014,

- 41(1): 0107001.  
 张金胜, 宁永强, 张金龙, 等. 大功率半导体激光器腔面膜的场强分布优化[J]. 中国激光, 2014, 41(1): 0107001.
- 8 Lundeberg L D A, Lousberg G P, Boiko D L, *et al.*. Spatial coherence measurements in arrays of coupled vertical cavity surface emitting lasers [J]. Appl Phys Lett, 2007, 90 (2): 021103.
- 9 Hao Yongqin, Yan Changling, Ma Xiaohui, *et al.*. Progress on single mode vertical cavity surface emitting lasers[J]. Laser & Optoelectronics Progress, 2013, 50(10): 100003.  
 郝永芹, 宴长岭, 马晓辉, 等. 单模垂直腔面发射激光器的研究动态[J]. 激光与光电子学进展, 2013, 50(10): 100003.
- 10 Ann C Lehman, Kent D Choquette. In-phase evanescent coupled implant defined vertical cavity laser arrays [C]. 19th Annual Meeting of the IEEE, 2006. 446 - 447.
- 11 A C Lehman, D F Siriani, K D Choquette. Two-dimensional electronic beam-steering with implant-defined coherent VCSEL arrays[J]. Electron Lett, 2007, 43(22): 1202 - 1203.
- 12 Liu Simin, Xu Jingjun, Guo Ru. Principle and Application of Coherent Optics [M]. 1st Editon. Tianjing: Nankai University Press, 2001. 2 - 16.  
 刘思敏, 许京军, 郭 儒. 相干光学原理及应用[M]. 第一版. 天津: 南开大学出版社, 2001. 2 - 16.
- 13 B J Thompson, E Wolf. Two-beam interference with partially coherent light[J]. J Opt Soc Am, 1957, 47(10): 895 - 902.
- 14 J Perina. Coherent of Light [M]. 1st Edition. Dordrecht: D Reidel Publishing, 1985. 24 - 37.
- 15 E Wolf, M Born. Principles of Optics[M]. 7th Edition. London: Cambridge University Press, 1999. 562 - 589.
- 16 W Leitenberger, S M Kuznetsov, A Snigirev. Interferometric measurements with hard X-rays using a double slit [J]. Opt Commun, 2011, 191(1-2): 91 - 96.
- 17 Zhao Kaihua, Zhong Xihua. Optics [M]. 1st Edition. Beijing: Peking University Press, 1984. 7 - 10 (part ii).  
 赵凯华, 钟锡华. 光学[M]. 第一版. 北京: 北京大学出版社, 1984. 7 - 10 (下册).

栏目编辑: 何卓铭